NASA TECHNICAL NOTE

NASA TN D-6703

EVALUATION OF THE USE OF A SINGULARITY ELEMENT IN FINITE-ELEMENT ANALYSES OF CENTER-CRACKED PLATES

by Alexander Mendelson, Bernard Gross, and John E. Srawley

Lewis Research Center
Cleveland, Ohio 44135

NATIONAL AERONAUTICS AND SPACE ADMINISTRATION • WASHINGTON, D. C. • MARCH 1972

1. Report No.	2. Government Accession No.	3. Recipient's Catalog No.
NASA TN D-6703		

4. Title and Subtitle	5. Report Date
EVALUATION OF THE USE OF A SINGULARITY ELEMENT IN FINITE-ELEMENT ANALYSES OF CENTER-CRACKED PLATES	March 1972
	6. Performing Organization Code
7. Author(s)	8. Performing Organization Report No.
Alexander Mendelson, Bernard Gross, and John E. Srawley	E-6680
	10. Work Unit No.
9. Performing Organization Name and Address	134-03
Lewis Research Center National Aeronautics and Space Administration Cleveland, Ohio 44135	11. Contract or Grant No.
	13. Type of Report and Period Covered
12. Sponsoring Agency Name and Address	Technical Note
National Aeronautics and Space Administration Washington, D.C. 20546	14. Sponsoring Agency Code

15. Supplementary Notes

16. Abstract

Two different methods are applied to the analyses of finite width linear elastic plates with central cracks. Both methods give displacements as a primary part of the solution. One method makes use of Fourier transforms. The second method employs a coarse mesh of triangular second-order finite elements in conjunction with a single singularity element subjected to appropriate additional constraints. The displacements obtained by these two methods are in very good agreement. These results suggest considerable potential for the use of a cracked element for related crack problems, particularly in connection with the extension to nonlinear material behavior.

17. Key Words (Suggested by Author(s))	18. Distribution Statement
Crack displacements Singularity elements Finite elements	Unclassified - unlimited

19. Security Classif. (of this report)	20. Security Classif. (of this page)	21. No. of Pages	22. Price*
Unclassified	Unclassified	23	$3.00

* For sale by the National Technical Information Service, Springfield, Virginia 22151

EVALUATION OF THE USE OF A SINGULARITY ELEMENT IN FINITE-ELEMENT ANALYSES OF CENTER-CRACKED PLATES

by Alexander Mendelson, Bernard Gross, and John E. Srawley

Lewis Research Center

SUMMARY

Two different methods are applied to the analyses of finite width linear elastic plates with central cracks. Both methods give displacements as a primary part of the solution. One method makes use of Fourier transforms. The second method employs a coarse mesh of triangular second-order finite elements in conjunction with a single singularity element subjected to appropriate additional constraints. The displacements obtained by these two methods are in very good agreement. These results suggest considerable potential for the use of a cracked element for related crack problems, particularly in connection with the extension to nonlinear material behavior.

INTRODUCTION

The purpose of this study was to compare results of two methods of numerical analysis that model the deformation of cracks in two-dimensional bodies of linear elastic materials. The study is preliminary to the further development of a hybrid finite-element method for application to cracked bodies of nonlinear materials. The hybrid method employs a special crack-tip element that can be designed to satisfy a variety of conditions. It was considered necessary first to evaluate the accuracy of the hybrid method for linear material behavior by comparison with an inherently more accurate method that makes use of Fourier transforms and satisfies compatibility and equilibrium throughout the body. The two methods were applied to centercracked plates of finite width for which linear elastic stress intensity coefficients have been obtained with high accuracy by several investigators (refs. 1 to 4).

The Fourier transform method reduces the problem to the solution of a pair of Fredholm integral equations that can be solved by a simple iterative process which is rapidly convergent. The advantages of the method are that the crack surface displace-

ments are a direct result of the solution of the integral equations, the stress (and strain) distributions are given by simple quadratures, and the required computational program is fairly simple. The ordinary finite-element method is inherently unsatisfactory for resolution of displacements very near to the crack tip because of its essentially discrete nature. The introduction of a finite element that itself contains a crack (ref. 5), called a singularity element (ref. 6), avoids this difficulty, but at the cost of loss of conditions of interelement continuity of displacement. In the present study a crack tip element of the inverse square root singularity type was incorporated into a coarse mesh of second-order elements to model the deformation of the crack and compute stress intensity coefficients. The results compare quite favorably with those of the Fourier transform method, and thus lend confidence in the further development of the hybrid method for application to nonlinear material behavior (which will require a different kind of crack tip element, however).

SYMBOLS

2a	crack length
B	plate thickness
2b	plate width
[D]	elastic matrix for plane strain conditions
FT	Fourier transform method
FE	finite element method
G	shear modulus
K_I	stress intensity factor, mode I
[k]	element stiffness matrix
2L	plate length
N	mesh density, number of finite elements per unit area
{P}	nodal force column vector
r, θ	polar coordinates
S_y, S_x, S_{xy}	dimensionless stress
[T]	displacement matrix
{U}	displacement column vector
u, v	displacements in x and y directions

v_o	uniform end displacement of plate
x, y	dimensionless cartesian coordinates with respect to b
$[\Gamma]$	strain matrix
$\{\epsilon\}$	strain column vector
$\epsilon_y, \epsilon_x, \gamma_{xy}$	components of strain column vector
λ	plate length to plate width ratio
μ	Poissons ratio
ν, ξ	dummy integration variables
$\{\sigma\}$	stress column vector
$\sigma_y, \sigma_x, \tau_{xy}$	components of stress column vector
$\{\ \}$	column vector, $m \times 1$
$[\ ]$	matrix, $m \times m$

FOURIER TRANSFORM SOLUTION

We consider the plane stress solution for an infinite strip loaded in tension. The strip is two units wide and contains a central crack of length 2a. Because of the symmetry we need consider only one quadrant such as the upper right quadrant. The details of the solution are given in appendix A. Here, we summarize the equations and method used in the computations. If v(x, 0) is the displacement along the crack, then, as shown in appendix A, the following equations must be satisfied:

$$v(x, 0) = \int_0^{a/b} v(\nu, 0)K\, d\nu + \int_0^{a/b} [1 + p(\nu)]K_1\, d\nu \tag{1}$$

here, v is the displacement of the crack divided by the ratio of the load to the elastic modulas and

$$Q(y) = -\pi \int_0^{a/b} v(\nu)\left(I_1 + y\frac{\partial I_1}{\partial y}\right)d\nu \tag{2}$$

where

$$\overline{Q}(\xi) = \int_0^{\infty} Q(y)\cos(\xi, y)dy \tag{3}$$

and

$$p(\nu) = \int_0^\infty \bar{Q}(\xi) K_2(\nu, \xi) d\xi \tag{4}$$

The functions K, K_1, K_2, and I_1 are given by equations (19), (18), (25), and (21) in appendix A.

The solution is obtained as follows. Assuming $p(\nu)$ equal to zero, equation (1) is solved for $v(x, 0)$. This is done by straightforward iteration since equation (1) is a simple Fredholm equation of the second kind, which converges very rapidly. Once $v(x, 0)$ is determined the integrations indicated in equations (2) to (4) are carried out successively to determine $p(\nu)$, which is then substituted into equation (1), and the process is repeated until there is no longer any significant change in either $v(x, 0)$ or $p(\nu)$. The whole process converges very rapidly, four or five iterations being sufficient for any engineering application.

Once the crack surface displacement is determined from the solution of equations (1) to (4), the stress at any point can be computed by simple quadrature as follows:

$$\left.\begin{aligned} S_x(x, y) &= 1 - \pi \int_0^{a/b} v(\nu, 0) \left(I_1 - \frac{\partial I_1}{\partial y} y \right) d\nu + \int_0^\infty \bar{Q}(\xi) K_3 \, d\xi \\ S_y(x, y) &= -\pi \int_0^{a/b} v(\nu, 0) \left(I_1 + y \frac{\partial I_1}{\partial y} \right) d\nu + \int_0^\infty \bar{Q}(\xi) K_2 \, d\xi \\ S_{xy}(x, y) &= \pi y \int_0^{a/b} v(\nu, 0) I_2 \, d\nu + \int_0^\infty \bar{Q}(\xi) K_4 \, d\xi \end{aligned}\right\} \tag{5}$$

where the functions I_1, I_2, K_2, K_3, and K_4 are given in the appendix. We note that in performing the numerical integrations in equation (1), a difficulty arises from the fact that the kernel $K(x, \nu)$ is singular at $\nu = a/b$. However, the principal value can be calculated as is shown in reference 7.

Figure 1 shows results obtained by this method (originally published in ref. 4). On the scale of this plot the individual values of the dimensionless stress intensity coefficient $2K_I Bb/Pa^{1/2}$ would be indistinguishable from the curve shown. Values taken from references 1 and 2 for comparison would also be indistinguishable from the curve. Further, results by this method are compared subsequently with results obtained by the finite-element method.

FINITE-ELEMENT ANALYSIS

Consider the plane elasto-static solution for a plate of finite dimensions, subject to a uniform end displacement. The plate has a central crack of length 2a and width 2b (fig. 2). Because of symmetry, we need consider only one quadrant. A mesh is generated of the type shown in figure 2(c). The stiffness matrices for the triangular and singular elements (fig. 3) are evaluated as shown in appendix B by the following equations:

$$[k]_{\substack{\text{Triangular}\\ \text{element}}} = B \iint_{\text{Area}} [\Gamma]^T [D][\Gamma] dA \tag{6}$$

$$[k]_{\substack{\text{Singular}\\ \text{element}}} = B\left[C^{-1}\right]^T \left(\iint_{\text{Area}} [\Gamma_1]^T [D][\Gamma_1] dA \right) [C^{-1}] \tag{7}$$

The matrices $[\Gamma]$, $[D]$, $[C]$, and $[\Gamma_1]$ are defined by equations (28), (29), (36), and (37) in appendix B.

The master stiffness matrix is then obtained by superimposing the various influence terms of the finite elements sharing common nodal points. The solution to the master stiffness matrix is then obtained by satisfying nodal equilibrium and boundary displacement conditions.

NUMERICAL RESULTS

The finite-element representation of the problem solved is shown in figures 2 and 3. The computational scheme is illustrated by the simple flow diagram as shown in figure 4. A comparison of dimensionless displacements along the crack quadrant surface is given in figure 5. As shown in these figures, the finite-element displacements compare favorably with that computed with the more accurate Fourier transform method. Because the Fourier transform method satisfied the conditions of compatibility and equilibrium throughout the strip, one would expect that the results of this approach to be more accurate. It is noteworthy that the Fourier transform results correspond to elliptical crack profiles in all three cases. Table I lists the Y stress intensity coefficients obtained herein and from references 3 and 5. Since displacements are the primary solution, the Y values were based on the computed nodal displacements. As the ratio λ decreased for a fixed number of elements (fig. 2), the comparison improved. This was primarily due to the fact that, as λ decreases the finite elements per unit

area, N (or mesh density) increases. The Y stress intensity coefficients showed a much greater sensitivity to the λ variation than the displacements.

As shown in figure 3, the location of the crack tip was always taken at the midpoints, between nodes 3 and 5. Node 4 was always taken at the midpoint between the crack tip and node 3. A preliminary study revealed that the results obtained by locating the crack tip ± 20 percent from the midpoint produced a small variation in the results. For larger changes in the crack tip location significant differences appeared.

Lewis Research Center,
National Aeronautics and Space Administration,
Cleveland, Ohio, December 1, 1971,
134-03.

APPENDIX A

FOURIER TRANSFORM ANALYSIS

We consider the problem of an infinite strip of width 2b and thickness B, containing a central crack of length 2a. The strip is loaded in tension with a tensile stress σ_∞, normal to the plane of the crack. The stresses and geometric variables are nondimensionalized in terms of σ_∞ and W, respectively. Because of symmetry, only one quadrant of the plate need be considered as shown in figure 6. The solution is obtained by the superposition of two solutions designated by A and B.

Problem A consists of a plate with a central crack, a tensile load at infinity, a normal load p(x) along the crack surface, and a self-equilibrating side load Q(y) at x = 1 (fig. 6). Problem B consists of a plate without a crack and without a load at infinity, but with a side load -Q(y) at x = 1 (fig. 6). By superposing the solutions to both these problems with the proper choice of Q(y) one obtains the desired solution to the problem of figure 6.

The solution to problem A can be obtained as follows. The equilibrium and compatibility equations for the plane problem of elasticity are

$$\left.\begin{aligned} \frac{\partial S_x}{\partial x} + \frac{\partial S_{xy}}{\partial y} &= 0 \\ \frac{\partial S_y}{\partial y} + \frac{\partial S_{xy}}{\partial x} &= 0 \\ \left(\frac{\partial^2}{\partial x^2} + \frac{\partial^2}{\partial y^2}\right)(S_x + S_y) &= 0 \end{aligned}\right\} \tag{8}$$

Applying a Fourier sine transform to the first of these equations and Fourier cosine transforms to the last two, solving the resulting ordinary differential equations and then taking the inverse transforms results, as shown in detail in reference 7, in

$$\left.\begin{aligned} S_y &= 1 + 2\sum_{m=1}^{\infty} A_m(1 + m\pi y)e^{-m\pi y}\cos m\pi x \\ S_x &= 2\sum_{m=1}^{\infty} A_m(1 - m\pi y)e^{-m\pi y}\cos m\pi x \\ S_{xy} &= 2\pi y\sum_{m=1}^{\infty} mA_m\, e^{-m\pi y}\sin m\pi x \end{aligned}\right\} \tag{9}$$

That equations (9) indeed satisfy equations (8) can be verified by direct substitution.

The displacements can now be calculated from the usual stress-strain relations and strain displacement results resulting for the case of plane stress in

$$v = \int_0^{a/b} v(\nu, y)d\nu - \frac{2}{\pi}\sum_{m=1}^{\infty}\frac{A_m}{m}[2 + (1 + \mu)m\pi y]e^{-m\pi y}\cos m\pi x \tag{10}$$

Along the plane of the crack (y = 0)

$$\left.\begin{aligned} S_y(x, 0) &= 1 + 2\sum_{m=1}^{\infty} A_m\cos m\pi x \\ \text{and} \\ v(x, 0) &= \int_0^{a/b} v(\nu, 0)d\nu - \frac{4}{\pi}\sum_{m=1}^{\infty}\frac{A_m}{m}\cos m\pi x \end{aligned}\right\} \tag{11}$$

Since equations (11) represent Fourier series expansions, it follows that

$$A_m = \int_0^1 S_y(\xi, 0)\cos m\pi\xi\, d\xi \tag{12}$$

and also

$$A_m = -\frac{m\pi}{2}\int_0^{a/b} v(\nu, 0)\cos m\pi\nu\, d\nu \tag{13}$$

The upper limit of integration in equation (13) follows from the fact that

$$v(\nu, 0) = 0, \qquad \frac{a}{b} \leq x \leq 1$$

Assuming a normal stress distribution p(x) along the crack surface, equation (12) can be written

$$A_m = \int_0^{a/b} p(\xi)\cos m\pi\xi \, d\xi + \int_{a/b}^{1} \sigma_y(\xi, 0)\cos m\pi\xi \, d\xi \tag{14}$$

Now, substituting (14) into the second of equations (11) and equation (13) into the first of equations (11) results in

$$v(x, 0) = \int_0^{a/b} v(\nu, 0)d\nu + \frac{1}{\pi}\int_0^{a/b} p(\nu)\ln\left[4(\cos \pi\nu - \cos \pi x)^2\right]d\nu$$

$$+ \frac{1}{\pi}\int_{a/b}^{1} S_y(\xi, 0)\ln\left[4(\cos \pi\xi - \cos \pi x)^2\right]d\xi \tag{15}$$

where

$$S_y(\xi, 0) = 1 + \frac{\pi}{2}\int_0^{a/b} v(\nu, 0) \frac{1 - \cos \pi\nu \cos \pi\xi}{(\cos \pi\nu - \cos \pi\xi)^2} \, d\nu \tag{16}$$

and where the following identities have been used

$$\left.\begin{aligned} \sum_{m=1}^{\infty} \frac{1}{m} \cos m\pi\nu \cos m\pi x &\equiv -\frac{1}{4}\ln\left[4(\cos \pi\nu - \cos \pi x)^2\right] \\ \sum_{m=1}^{\infty} m \cos m\pi\nu \cos m\pi\xi &\equiv -\frac{1}{2}\frac{1 - \cos \pi\nu \cos \pi\xi}{(\cos \pi\nu - \cos \pi\xi)^2} \end{aligned}\right\} \tag{17}$$

The first identity in equations (17) can be found for example in reference 8 (p. 358). The second can be obtained by differentiating the first one twice. It is obvious of course

that the second sum is divergent. Whether the formal sum given has meaning can only be ascertained from the final answer, which in this case can be shown by direct substitution to satisfy the equations of equilibrium and compatibility.

Finally substituting equation (16) into (15) gives

$$v(x,0) = \int_0^{a/b} [1+p(\nu)]K_1 \, d\nu + \int_0^{a/b} v(\nu,0)K \, d\nu$$

where

$$K_1 = \frac{1}{\pi} \ln\left[4(\cos \pi\nu - \cos \pi x)^2\right] \tag{18}$$

$$K = a + \frac{\sin \pi \frac{a}{b} \ln\left[4 \sin \frac{\pi\left(\frac{a}{b} + x\right)}{2} \sin \frac{\pi\left(\frac{a}{b} - x\right)}{2}\right]}{2\pi \sin \frac{\pi\left(\frac{a}{b} + \nu\right)}{2} \sin \frac{\pi\left(\frac{a}{b} - \nu\right)}{2}} - \frac{\sin \pi\nu \left[\ln \sin \frac{\pi\left(\frac{a}{b} + \nu\right)}{2} - \ln \sin \frac{\pi\left(\frac{a}{b} - \nu\right)}{2}\right]}{2\pi \sin \frac{\pi(x+\nu)}{2} \sin \frac{\pi(x-\nu)}{2}}$$

$$+ \frac{\sin \pi x \left[\ln \sin \frac{\pi\left(\frac{a}{b} + x\right)}{2} - \ln \sin \frac{\pi\left(\frac{a}{b} - x\right)}{2}\right]}{2\pi \sin \frac{\pi(x+\nu)}{2} \sin \frac{\pi(x-\nu)}{2}} \tag{19}$$

For a given pressure distribution $p(\nu)$ along the crack, equation (1) represents a Fredholm equation of the second kind. It can be solved by a straightforward iteration which converges very rapidly.

Once the crack opening is determined by the solution of equation (1), the stress distribution can be obtained by direct numerical integration as follows: Substituting equation (13) into equation (9), reversing the order of integration and summation, and formally summing the resulting infinite series give

$$\left.\begin{aligned} S_y(x, y) &= 1 - \pi \int_0^{a/b} v(\nu, 0)\left(I_1 - y\frac{\partial I_1}{\partial y}\right)d\nu \\ S_x(x, y) &= -\pi \int_0^{a/b} v(\nu, 0)\left(I_1 + y\frac{\partial I_1}{\partial y}\right)d\nu \\ S_{xy}(x, y) &= \pi y \int_0^{a/b} v(\nu, 0)\frac{\partial I_1}{\partial x}\,d\nu \end{aligned}\right\} \tag{20}$$

where

$$I_1 = \frac{1}{4}\left\{\frac{\cos \pi(\nu + x)\cosh \pi y - 1}{[\cos \pi(\nu + x) - \cosh \pi y]^2} + \frac{\cos \pi(\nu + x)\cosh \pi y - 1}{[\cos \pi(\nu - x) - \cosh \pi y]^2}\right\} \tag{21}$$

At the side boundary $x = 1$ we now have a self-equilibrating normal load

$$Q(y) \equiv S_x(1, y)$$

which can be computed from the second of equations (20). We have thus obtained a solution to problem A.

The solution to problem B is given in reference 9 (p. 412). For an infinite strip with a symmetric edge load $Q(y)$, we take the infinite Fourier transform

$$\overline{Q}(\xi) = \int_0^{\infty} Q(y)\cos(\xi, y)dy \tag{22}$$

Then the stresses are given by

$$S_x = \frac{4}{\pi}\int_0^\infty \bar{Q}(\xi)\,\frac{(\sinh\xi + \xi\cosh\xi)\cosh\xi x - \xi x \sinh\xi \sinh\xi x}{2\xi + \sinh 2\xi}\cos\xi y\, d\xi$$

$$S_y = \frac{4}{\pi}\int_0^\infty \bar{Q}(\xi)\,\frac{(\sinh\xi - \xi\cosh\xi)\cosh\xi x + \xi x \sinh\xi \sinh\xi x}{2\xi + \sinh 2\xi}\cos\xi y\, d\xi \qquad (23)$$

$$S_{xy} = \frac{4}{\pi}\int_0^\infty \bar{Q}(\xi)\,\frac{\xi x \sinh\xi \cosh\xi x - \xi \cosh\xi \sinh\xi x}{2\xi + \sinh 2\xi}\sin\xi y\, d\xi$$

Now at $y = 0$ this solution gives a stress in the y direction given by the second of equations (23)

$$p(\nu) \equiv S_y(x, 0) = \int_0^\infty \bar{Q}(\xi) K_2(\nu, \xi) d\xi \qquad 0 \le \nu \le \frac{a}{b} \qquad (24)$$

where

$$K_2 = \frac{4}{\pi}\,\frac{(\sinh\xi - \xi\cosh\xi)\cosh\xi\nu + \xi\nu \sinh\xi \sinh\xi\nu}{2\xi + \sinh 2\xi} \qquad (25)$$

By combining the solutions of problems A and B we can obtain a solution in which both the side loads $Q(y)$ and the normal loads on the crack surface cancel. This can be done by the simple iterative procedure described in the body of the report.

APPENDIX B

FINITE ELEMENT ANALYSIS

In the following analysis it is assumed that the body forces are negligible and that the model material is homogeneous and isotropic, has a constant thickness, and is subjected to plane strain elastostatic conditions. Define

$$\{U\} \equiv \begin{Bmatrix} v \\ u \end{Bmatrix}; \qquad \{\delta\} \equiv \begin{Bmatrix} v_1 \\ v_2 \\ \cdot \\ \cdot \\ \cdot \\ v_6 \\ u_1 \\ u_2 \\ \cdot \\ \cdot \\ \cdot \\ u_6 \end{Bmatrix}; \qquad \{\epsilon\} \equiv \begin{Bmatrix} \epsilon_y \\ \epsilon_x \\ \gamma_{xy} \end{Bmatrix} = \begin{Bmatrix} \dfrac{\partial v}{\partial y} \\ \dfrac{\partial u}{\partial x} \\ \dfrac{\partial v}{\partial x} + \dfrac{\partial u}{\partial y} \end{Bmatrix}; \qquad \{\sigma\} = \begin{Bmatrix} \sigma_y \\ \sigma_x \\ \tau_{xy} \end{Bmatrix} \tag{26}$$

Thus, we can also write

$$\{U\} = [T]\{\delta\} \tag{27}$$

$$\{\epsilon\} = [\Gamma]\{\delta\} \tag{28}$$

$$\{\sigma\} = [D]\{\epsilon\} = [D][\Gamma]\{\delta\} \tag{29}$$

Imposing virtual displacements at the element nodal points and equating the work done by by nodal force $\{P\}$ to the internal work done by the stress $\{\sigma\}$ (ref. 10), we obtain

$$\left\{\delta^v\right\}^T \{P\} = B \iint_{\text{area}} \left\{\epsilon^v\right\}^T \{\sigma\}\, dA$$

where superscript v refers to virtual and T to transpose. Substituting equation (29) and (28) into the last equation and comparing coefficients yields

$$\{P\} = B\left(\iint_{\text{area}} [\Gamma]^T[D][\Gamma]dA\right)\{\delta\}$$

Hence,

$$\{P\} = [k]\{\delta\} \tag{30}$$

where

$$[k] = B \iint_{\text{area}} [\Gamma]^T[D][\Gamma]dA \tag{31}$$

The typical triangular element as shown in figure 3 is assumed to be a second-order element. The displacement functions are as follows:

$$v(x, y) = \sum_{m=1}^{6} W_m(x, y)v_m$$

$$u(x, y) = \sum_{m=1}^{6} W_m(x, y)u_m$$

where

$$W_m(x, y) = a_{1,m} + a_{2,m}x + a_{3,m}y + a_{4,m}x^2 + a_{5,m}xy + a_{6,m}y_2$$

The constants $a_{i,m}$, $i = 1, 2, \ldots, 6$ are evaluated such that, at location (x_m, y_m) of node m, $W_m(x_m, y_m) = 1$ and $W_m(x_l, y_l) = 0$ at the remaining l nodal points. Thus $[T(x, y)]$ is obtained. The element stiffness matrix is evaluated in a manner similar to that in reference 11.

For the singularity element as shown in figure 3 the displacement functions, taken from references 12 and 13, are assumed to have the general form

$$\left.\begin{aligned} v(r, \theta) &= \frac{1}{2G}\left[\sum_{n=1}^{12} d_n r^{n/2} f_n(n, \theta)\right] \\ u(r, \theta) &= \frac{1}{2G}\left[\sum_{n=1}^{12} d_n r^{n/2} g_n(n, \theta)\right] \end{aligned}\right\}$$

For odd values of n

$$\left.\begin{aligned} f_n(n,\theta) &= F_1(n,\theta)\sin\theta + F_2(n,\theta)\cos\theta \\ g_n(n,\theta) &= F_1(n,\theta)\cos\theta - F_2(n,\theta)\sin\theta \end{aligned}\right\} \tag{32}$$

where

$$\left.\begin{aligned} F_1(n,\theta) &= \left(\frac{7}{2} - n - 4\mu\right)\cos\left(n - \frac{3}{2}\right)\theta + \left(n - \frac{3}{2}\right)\cos\left(n + \frac{1}{2}\right)\theta \\ \text{and} \\ F_2(n,\theta) &= \left(\frac{5}{2} + n - 4\mu\right)\sin\left(n - \frac{3}{2}\right)\theta - \left(n - \frac{3}{2}\right)\sin\left(n + \frac{1}{2}\right)\theta \end{aligned}\right\} \tag{33}$$

for even values of n

$$\left.\begin{aligned} f_n(n,\theta) &= F_3(n,\theta)\sin\theta + F_4(n,\theta)\cos\theta \\ g_n(n,\theta) &= F_3(n,\theta)\cos\theta - F_4(n,\theta)\sin\theta \end{aligned}\right\} \tag{34}$$

where

$$\left.\begin{aligned} F_3(n,\theta) &= (3 - n - 4\mu)\cos(n-1)\theta + (n+1)\cos(n+1)\theta \\ \text{and} \\ F_4(n,\theta) &= -(3 + n - 4\mu)\sin(n-1)\theta + (n+1)\sin(n+1)\theta \end{aligned}\right\} \tag{35}$$

To obtain the singularity element stiffness matrix, the element is divided into many (p) segments. A typical segment is shown in figure 3. From equation (27) in matrix formulation we have

$$\{U\} = [H]\{d\}$$

At the six nodal points we evaluate

$$\{\delta\} = [C]\{d\} \tag{36}$$

hence

$$\{d\} = [C^{-1}]\{\delta\}$$

thus

$$\{U\} = [H][C^{-1}]\{\delta\}$$

And from equation (28)

$$\{\epsilon\} = [\Gamma_1]\{d\} = [\Gamma_1][C^{-1}]\{\delta\} \tag{37}$$

and it follows that

$$[k]_{\substack{\text{singularity}\\ \text{element}}} = B\left[C^{-1}\right]^T\left(\iint_{\text{area}} [\Gamma_1]^T[D][\Gamma_1]dA\right)[C^{-1}] \tag{38}$$

Let

$$[P_{q,t}] = \iint_{\text{area}} [\Gamma^T][D][\Gamma]dA$$

After some algebraic manipulation and integration the matrix elements become

$$P_{q,t} = \sum_{j=1}^{p}\sum_{s=1}^{3}\sum_{z=1}^{3} \frac{2}{q+t} r_j^{(q+t)/2}\left[G_{z,q}(\theta_j)D_{z,s}G_{s,t}(\theta_j)\right]\Delta\theta_j \tag{39}$$

where $q, t = 1, 2, \ldots, 12$, p is the number of segments of the cracked element, and

$$
\left.
\begin{aligned}
G(\theta)_{1,\,2n-1} &= F_1(n,\theta)(X_1 \sin^2\theta + \cos^2\theta) + F_2(n,\theta)X_2 \sin\theta\cos\theta + F'_1(n,\theta)\sin\theta\cos\theta + F'_2(n,\theta)\cos^2\theta \\
G(\theta)_{2,\,2n-1} &= F_1(n,\theta)(X_1 \cos^2\theta + \sin^2\theta) - F_2(n,\theta)X_2 \sin\theta\cos\theta - F'_1(n,\theta)\sin\theta\cos\theta + F'_2(n,\theta)\sin^2\theta \\
G(\theta)_{3,\,2n-1} &= F_1(n,\theta)X_2 \sin 2\theta + F_2(n,\theta)X_2 \cos 2\theta + F'_1(n,\theta)\cos 2\theta - F'_2(n,\theta)\sin 2\theta \\
G(\theta)_{1,\,2n} &= F_3(n,\theta)(n \sin^2\theta + \cos^2\theta) + F_4(n,\theta)X_3 \sin\theta\cos\theta + F'_3(n,\theta)\sin\theta\cos\theta + F'_4(n,\theta)\cos^2\theta \\
G(\theta)_{2,\,2n} &= F_3(n,\theta)(n \cos^2\theta + \sin^2\theta) - F_4(n,\theta)X_3 \sin\theta\cos\theta - F'_3(n,\theta)\sin\theta\cos\theta + F'_4(n,\theta)\sin^2\theta \\
G(\theta)_{3,\,2n} &= F_3(n,\theta)X_3 \sin 2\theta + F_4(n,\theta)X_3 \cos 2\theta + F'_3(n,\theta)\cos 2\theta - F'_4(n,\theta)\sin 2\theta
\end{aligned}
\right\} \quad (40)
$$

where

$$X_1 = n - \frac{1}{2}$$

$$X_2 = n - \frac{3}{2}$$

$$X_3 = (n - 1)$$

and

$$\frac{d}{d\theta}\left[F(n,\theta)\right] = F'(n,\theta)$$

REFERENCES

1. Isida, M.: Stress-Intensity Factors for the Tension of an Eccentrically Cracked Strip. J. Appl. Mech., vol. 33, no. 3, Sept. 1966, pp. 674-675.

2. Forman, R. G.; and Kobayashi, A. S.: On the Axial Rigidity of Perforated Strip and the Strain Energy Release Rate in a Centrally Notched Strip Subjected to Uniaxial Tension. J. Basic Eng., vol. 86, no. 4, Dec. 1964, pp. 693-699.

3. Sneddon, I. N.; and Srivastav, R. P.: The Stress Field in the Vicinity of a Griffith Crack in a Strip of Finite Width. Int. J. Eng. Sci., vol. 9, no. 5, May 1971, pp. 479-488.

4. Brown, W. F., Jr.; and Srawley, J. E.: Plane Strain Crack Toughness Testing of High Strength Metallic Materials. Spec. Tech. Publ. No. 410, ASTM, 1967.

5. Byskov, Esben: The Calculation of Stress Intensity Factors Using the Finite Element Method with Cracked Elements. Int. J. Fracture Mech., vol. 6, no. 2, June 1970, pp. 159-167.

6. Gallagher, R. H.: Survey and Evaluation of the Finite Element Method in Fracture Mechanics Analysis. Presented at the First International Conference on Structural Mechanics in Reactor Technology, Berlin, West Germany, Sept. 1971.

7. Mendelson, Alexander; and Spero, Samuel W.: Elastic Stress Distribution in a Finite-Width Orthotropic Plate Containing a Crack. NASA TN D-2260, 1964.

8. Bromwich, T. J. I'A.: An Introduction to the Theory of Infinite Series. Second ed., rev., Macmillan Co., 1926.

9. Sneddon, Ian N : Fourier Transforms. McGraw-Hill Book Co., Inc., 1951.

10. Zienkiewicz, O. C.; and Cheung, Y. K.: The Finite Element Method in Structural and Continuum Mechanics. McGraw-Hill Book Co., Inc., 1967.

11. de Veubeke, B. F.: Displacement and Equilibrium Models in the Finite Element Method. Stress Analysis. O. C. Zienkiewicz and G. S. Holister, eds., John Wiley & Sons, Inc., 1965, pp. 145-197.

12. Williams, M. L.: On the Stress Distribution at the Base of a Stationary Crack. J. Appl. Mech., vol. 24, no. 1, Mar. 1957, pp. 109-114.

13. Gross, Bernard; Roberts, Ernest, Jr.; and Srawley, John E.: Elastic Displacements for Various Edge-Cracked Plate Specimens. Int. J. Fracture Mech., vol. 4, no. 3, Sept. 1968, pp. 267-276 (errata, vol. 6, 1970, p. 87.)

TABLE I. - DIMENSIONLESS STRESS INTENSITY COEFFICIENTS FOR VARIOUS NOTCH DEPTH TO PLATE WIDTH RATIOS AND MESH DENSITY

Method	Source	Mesh density, N	Notch depth to plate width ratio, a/b			
			0.1	0.3	0.333	0.305
			Dimensionless stress intensity coefficient, $Y = (2bBK_I)/(P\sqrt{a})$			
Fourier transform	This report	--	1.78	1.87	1.90	2.11
	Ref. 3	--	1.79	1.88	----	2.12
Finite element	Ref. 5	(a)	----	----	1.83	----
	This report	16	----	----	1.74	----
		18	----	----	----	2.08
		21	----	1.79	1.81	----
		32	1.52	1.82	----	----
		64	1.66	----	----	----
		80	1.65	----	----	----

[a]Not available.

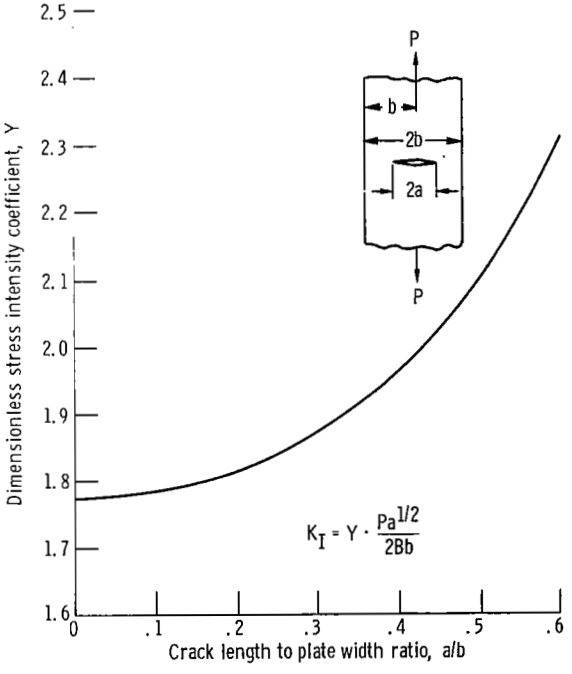

Figure 1. - Stress calibrations for center-cracked specimen (refs. 1, 2, and 7).

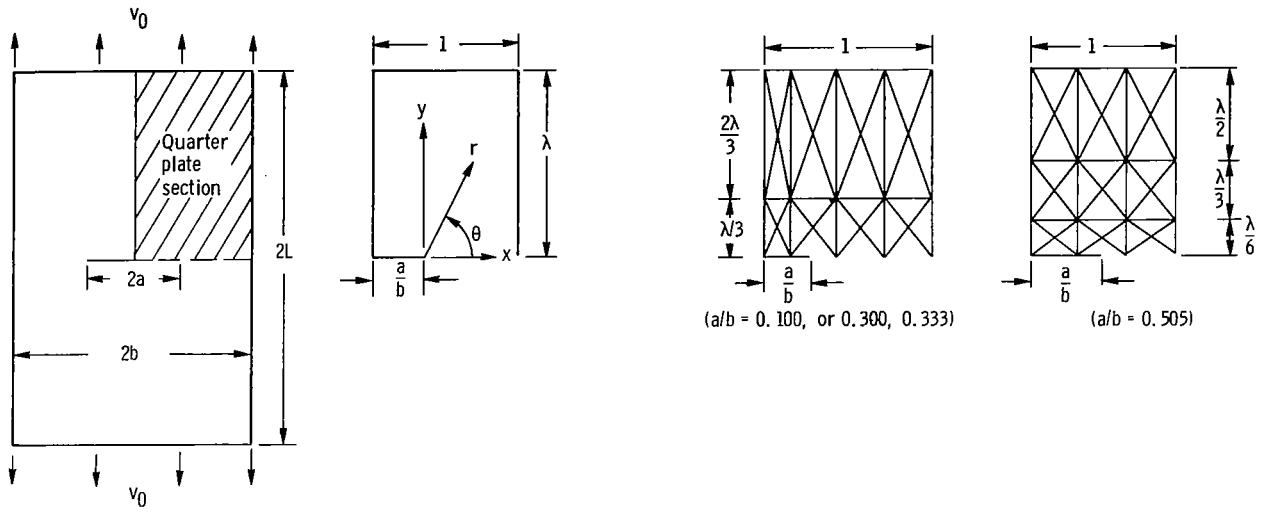

(a) Center cracked plate subjected to uniform end displacement, V_0.

(b) Dimensionless quarter section.

(c) Typical finite-element mesh for quarter section.

Figure 2. - Plate configuration and typical finite-element mesh.

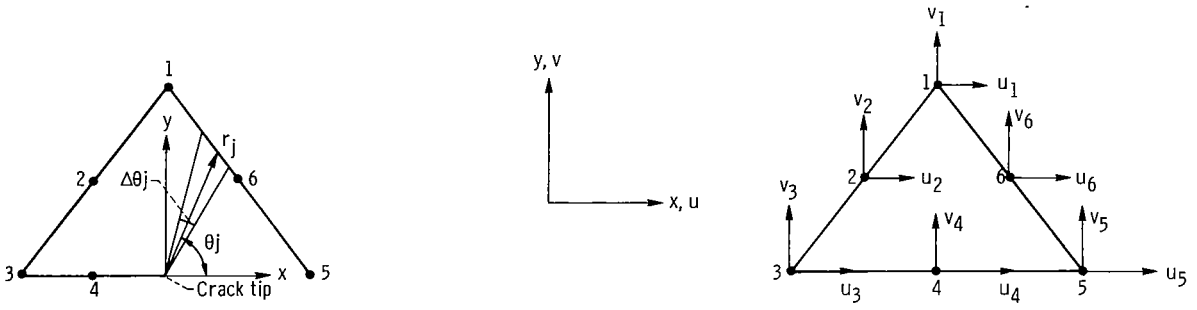

Crack element with node locations at verticies and midpoints and typical segment used for numerical integration

Typical 2nd order triangular element with node locations at verticies and midpoints

Figure 3. - Typical finite-elements for center cracked plate.

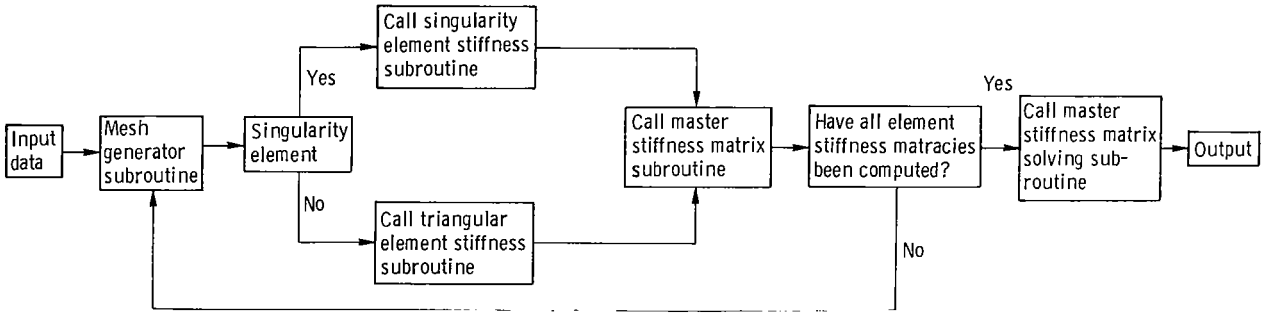

Figure 4. - Simplified flow diagram of program operations.

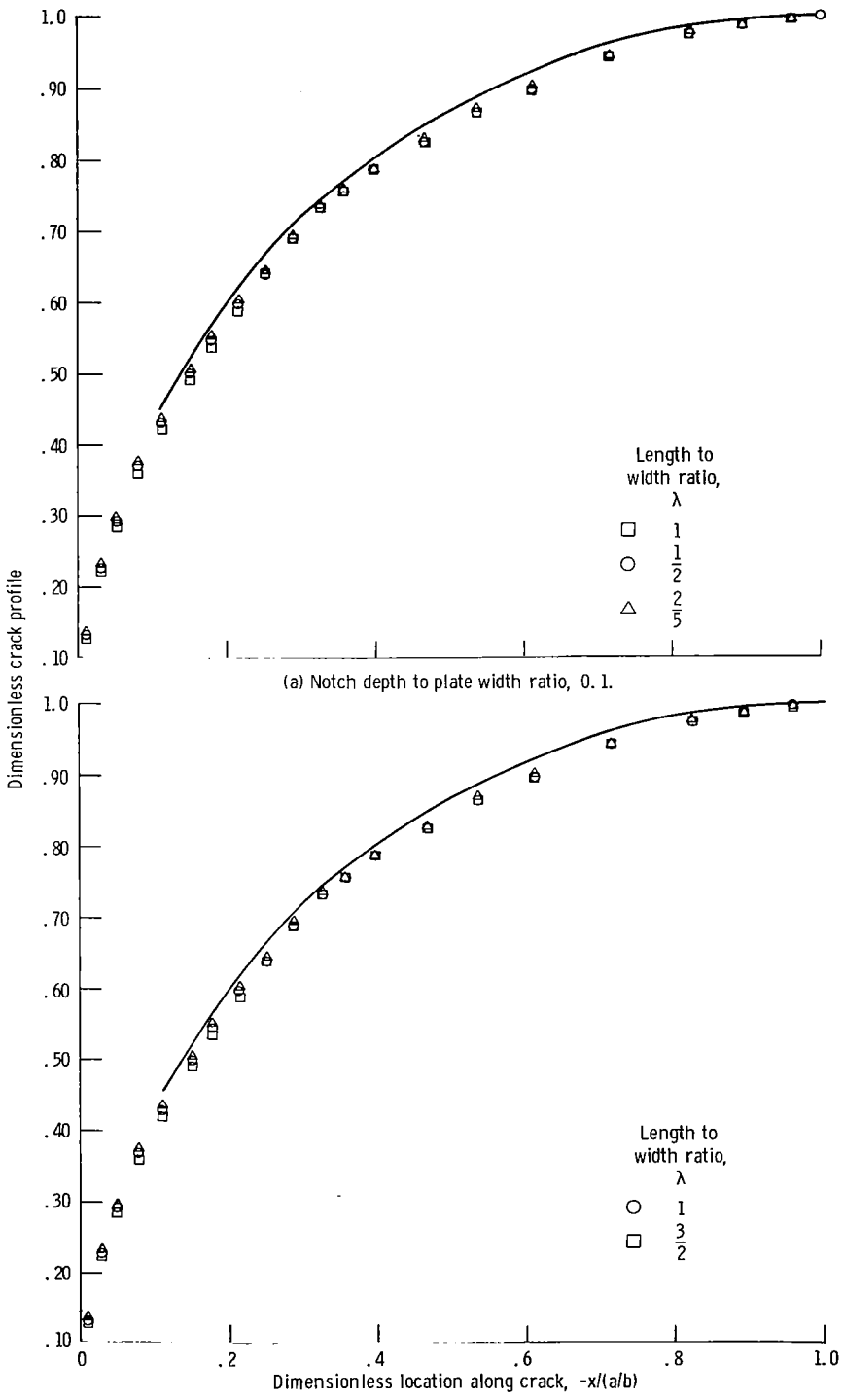

Figure 5. - Crack displacement profile for various length to width ratios.

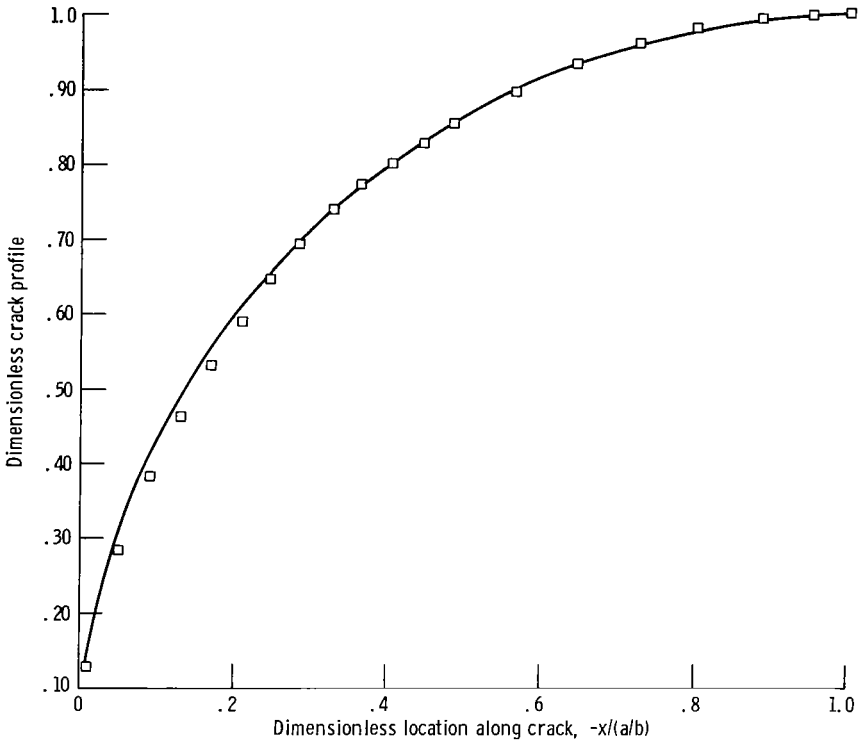

(c) Notch depth to plate width ratio, 0.5. Length to width ratio, 2.

Figure 5. - Concluded.

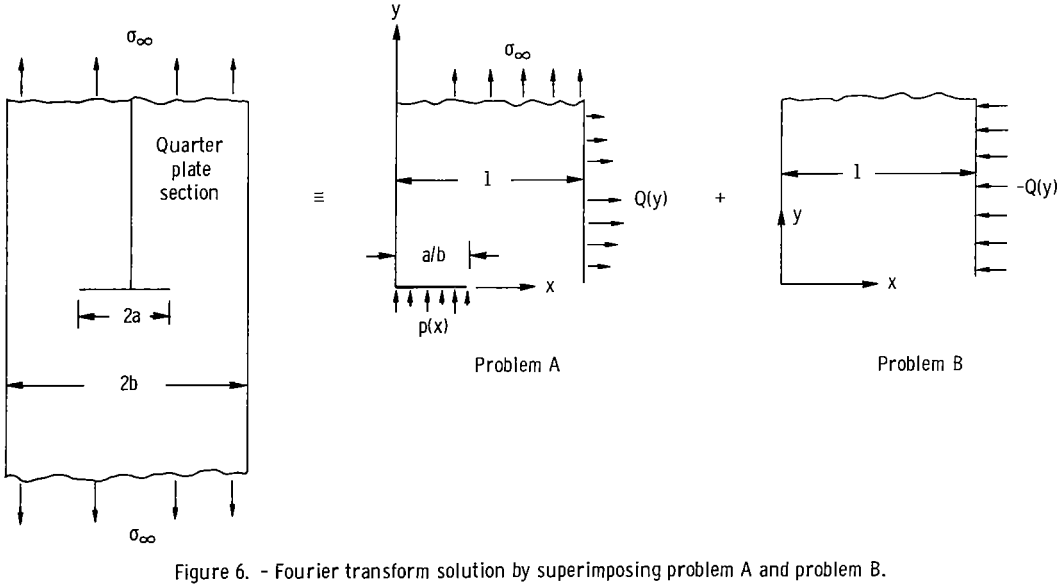

Figure 6. - Fourier transform solution by superimposing problem A and problem B.

"The aeronautical and space activities of the United States shall be conducted so as to contribute . . . to the expansion of human knowledge of phenomena in the atmosphere and space. The Administration shall provide for the widest practicable and appropriate dissemination of information concerning its activities and the results thereof."

—NATIONAL AERONAUTICS AND SPACE ACT OF 1958

NASA SCIENTIFIC AND TECHNICAL PUBLICATIONS

TECHNICAL REPORTS: Scientific and technical information considered important, complete, and a lasting contribution to existing knowledge.

TECHNICAL NOTES: Information less broad in scope but nevertheless of importance as a contribution to existing knowledge.

TECHNICAL MEMORANDUMS: Information receiving limited distribution because of preliminary data, security classification, or other reasons.

CONTRACTOR REPORTS: Scientific and technical information generated under a NASA contract or grant and considered an important contribution to existing knowledge.

TECHNICAL TRANSLATIONS: Information published in a foreign language considered to merit NASA distribution in English.

SPECIAL PUBLICATIONS: Information derived from or of value to NASA activities. Publications include conference proceedings, monographs, data compilations, handbooks, sourcebooks, and special bibliographies.

TECHNOLOGY UTILIZATION PUBLICATIONS: Information on technology used by NASA that may be of particular interest in commercial and other non-aerospace applications. Publications include Tech Briefs, Technology Utilization Reports and Technology Surveys.

Details on the availability of these publications may be obtained from:

SCIENTIFIC AND TECHNICAL INFORMATION OFFICE

NATIONAL AERONAUTICS AND SPACE ADMINISTRATION

Washington, D.C. 20546